AGU ADVANCING EARTH AND SPACE SCIENCES

Earth and Space Science

RESEARCH ARTICLE
10.1029/2023EA003378

Evaluation of Vertical Patterns in Chlorophyll-A Derived From a Data Assimilating Model of Satellite-Based Ocean Color

Lionel A. Arteaga[1,2] and **Cecile S. Rousseaux**[3]

[1]Global Modeling and Assimilation Office, NASA Goddard Space Flight Center, Greenbelt, MD, USA, [2]Goddard Earth Sciences, Technology and Research II, University of Maryland Baltimore County, Baltimore, MD, USA, [3]Ocean Ecology Laboratory, NASA Goddard Space Flight Center, Greenbelt, MD, USA

Abstract Satellite-based sensors of ocean color have become the primary tool to infer changes in surface chlorophyll, while BGC-Argo floats are now filling the information gap at depth. Here we use BGC-Argo data to assess depth-resolved information on chlorophyll-a derived from an ocean biogeochemical model constrained by the assimilation of surface ocean color remote sensing. The data-assimilating model replicates well the general seasonality and meridional gradients in surface and depth-resolved chlorophyll-a inferred from the float array in the Southern Ocean. On average, the model tends to overestimate float-based chlorophyll, particularly at times and locations of high productivity such as the beginning of the spring bloom, subtropical deep chlorophyll maxima, and non-iron limited regions of the Southern Ocean. The highest model RMSE in the upper 50 m with respect to the float array is of 0.6 mg Chl m^{-3}, which should allow the detection of seasonal changes in float-based biomass (varying between 0.01 and >1 mg Chl m^{-3}) but might hinder the identification of subtle changes in chlorophyll at narrow local scales. Both model and float profiling data show good agreement with in situ data from station ALOHA, with model estimates showing a slight accuracy edge in inferring depth-resolved observations. Uncertainties in float bio-optical estimates impede their use as a reliable benchmark for validation, but the general qualitative agreement between model and float data provides confidence in the ability of model to replicate biogeochemical features below the surface, where data is not directly constrained by the assimilation of satellite ocean color.

Plain Language Summary Changes in oceanic chlorophyll can indicate alterations in the biomass of photosynthetic algae, which sustain marine ecosystems and have the capacity to alter the climate system. Algae live not only in the surface of the ocean, where satellites can observe them, but also beneath the upper marine layer, where autonomous profiling systems (floats) are used to infer their vertical distribution. Here we use float profiling data to evaluate the representation of chlorophyll biomass with depth from a numerical ecosystem model informed by surface satellite information. Chlorophyll outputs from the model agree generally well with information from the floats in terms of timing and spatial representation of low and high chlorophyll areas. Overall, the model's chlorophyll concentrations are slightly higher than those indicated by the floats. However, float measurements are not perfect, as suggested by a localized comparison of both float and model chlorophyll profiles with field observations at various oceanic depths near the Hawaiian Islands. While neither float- nor model-based data produce perfect estimations of oceanic chlorophyll across all three dimensions, their general agreement suggests that the model is able to mimic biological and physical dynamics both at and below the ocean surface.

Key Points:

- Modeled vertical chlorophyll profiles obtained by assimilating satellite ocean color are compared against BGC-Argo and in situ data
- Model chlorophyll is higher but replicates well the general seasonality and meridional gradients of the BGC-Argo array in the Southern Ocean
- Mean chlorophyll profiles from the model tend to be in better agreement with in situ data at station ALOHA (~±50%) than float estimates

Supporting Information:

Supporting Information may be found in the online version of this article.

Correspondence to:

L. A. Arteaga,
lionel.arteagaquintero@nasa.gov

Citation:

Arteaga, L. A., & Rousseaux, C. S. (2024). Evaluation of vertical patterns in chlorophyll-a derived from a data assimilating model of satellite-based ocean color. *Earth and Space Science*, *11*, e2023EA003378. https://doi.org/10.1029/2023EA003378

Received 23 OCT 2023
Accepted 16 JUN 2024

Author Contributions:

Conceptualization: Lionel A. Arteaga
Formal analysis: Lionel A. Arteaga
Investigation: Lionel A. Arteaga
Methodology: Lionel A. Arteaga, Cecile S. Rousseaux
Software: Cecile S. Rousseaux
Validation: Lionel A. Arteaga
Visualization: Lionel A. Arteaga
Writing – original draft: Lionel A. Arteaga
Writing – review & editing: Lionel A. Arteaga, Cecile S. Rousseaux

1. Introduction

Chlorophyll is considered to be a an Essential Climate Variable (ECV) by the Global Climate Observing System (GCOS), deeming it a critical ecological marker to the characterization of changes in Earths's climate. Within the GCOS framework, the accurate estimation of chlorophyll is necessary for the monitoring of surface ocean color and phytoplankton biomas. Similarly, chlorophyll is a key component for the computation of marine primary productivity in a wide range of ocean color and numerical biogeochemical models (Behrenfeld & Falkowski, 1997; Carr et al., 2006; Laufkötter et al., 2015). The inference and potential prediction of major biological and geochemical metrics such as annual fish catches and air-sea fluxes of carbon dioxide hinge on the reliable estimation of oceanic chlorophyll (Landschützer et al., 2016; Park et al., 2019).

Space-based observations of ocean color are the primary tool employed to estimate surface ocean chlorophyll at the regional and global scale. The use of this technology began ∼40 years ago when retrievals from the Coastal Zone Color Scanner (CZCS) indicated that phytoplankton pigment concentrations diminished during 1982–1983 Niño (Feldman et al., 1984), providing one of the first evidence of oceanic biological effects associated to El Niño Southern Oscillation (ENSO) cycles. Satellite ocean color can provide repeated global coverage every 2–3 days at the equator and daily coverage at higher latitudes at a relatively high spatial resolution (pixel size ∼1–10 km) (IOCCG, 2008). However, ocean color remote sensing is hindered by its inability to retrieve information due to high solar zenith angle, clouds, aerosols, sun glint (Gregg & Casey, 2007b; IOCCG, 2020), and its retrievals are mostly restricted to the surface ocean or first optical depth. The lack of biogeochemical information at depth can be fulfilled with the increasingly growing network of biogeochemical (BGC)-Argo floats, many of which are now equipped with bio-optical sensors to infer biological signals such as chlorophyll-based fluorescence and particle backscattering (Chai et al., 2020; Claustre et al., 2020; Matsumoto et al., 2022; Riser et al., 2018). Most Argo floats tend to follow a quasi-lagrangian sampling pattern that needs to be taken into account when combining their profiling information with the more eulerian tendency of satellite-based products (Kuhn et al., 2023; McKee et al., 2022).

An alternative approach for expanding surface remote sensing information to depth is the incorporation of satellite ocean color into numerical models via data assimilation (DA). An example of such application is the NASA Ocean Biogeochemical Model (NOBM), which was developed with the goal of covering gaps and correcting remote sensing retrievals using mechanistic biogeochemical and ocean circulation dynamics. The assimilation of satellite ocean color improves surface estimates of chlorophyll relative to the free-run/non-assimilating implementation of the model. This improvement is evidenced by stark reductions in the bias and uncertainty of the model output with respect to satellite and in situ chlorophyll data, as well as primary productivity rates (Gregg, 2008). While the model's surface biogeochemical fields have been validated with respected to satellite and in situ data sets (Arteaga & Rousseaux, 2023; Gregg & Casey, 2007a; Gregg et al., 2003, 2014; Rousseaux & Gregg, 2015), the vertical structure of the model output has not been evaluated to date, mostly due to the lack of in situ biogeochemical profiles. Here, we describe the vertical structure in the NOBM's chlorophyll-a output and compare it with BGC-Argo float profiles from the Southern Ocean Carbon Climate and Modeling project (SOCCOM) and in situ data from the Hawaii Ocean Time-series (HOT) program, station ALOHA. Aside from this station, our comparison focuses primarily on the Southern Ocean given that this is the main regional target of the SOCCOM project and therefore has the highest density of consistently treated, high quality-controlled (QC) float profiling data. Our analysis shows a general qualitative agreement between float and model chlorophyll output in the Southern Ocean, with model estimates yielding on average slightly higher chlorophyll concentration than the float array. At station ALOHA, model-based profiles agree with in situ chlorophyll observations moderately better than float profiles. We discuss implications for seasonal and meridional patterns of depth-resolved chlorophyll in the Southern Ocean from both model and float profiles and potential caveats in both estimates.

2. Data

2.1. NASA Ocean Biogeochemical Model

The NOBM provides a numerical representation of nutrient, planktonic (phytoplankton and zooplankton), and detritus ecosystem dynamics (NPZD-type model), including characterization of carbonate-chemistry for the estimation of carbon fluxes (Gregg & Casey, 2007a; Gregg et al., 2014). The ecosystem model includes explicit representation of six phytoplankton functional types (PFTs) (diatoms, coccolithophores, chlorophytes, dinoflagellates, cyanobacteria, and phaeocystis), each of which respond differently to changes in the physical environment and compete for nutrient and light resources (Arteaga & Rousseaux, 2023; Rousseaux & Gregg, 2012) (see Tables S1 and S2 in Supporting Information S1 for specific light and nutrient uptake coefficient values). Phytoplankton growth is based on Monod's model (Michaelis-Menten kinetics). Grazing is enforced by a single zooplankton group, which feeds on PFTs proportionally to their relative abundance. This enables herbivore grazing to self-adapt to the prevailing phytoplankton community. The biogeochemical/ecosystem module is coupled within a three-dimensional ocean circulation model (Poseidon, Schopf & Loughe, 1995), which spans a near-global domain from 84°S to 72°N at a spatial resolution of 1.25° longitude and $\frac{2}{3}^{\circ}$ latitude, contains 14 vertical layers in quasi-isopycnal coordinates, and is restricted to waters deeper than 200 m. The light field is

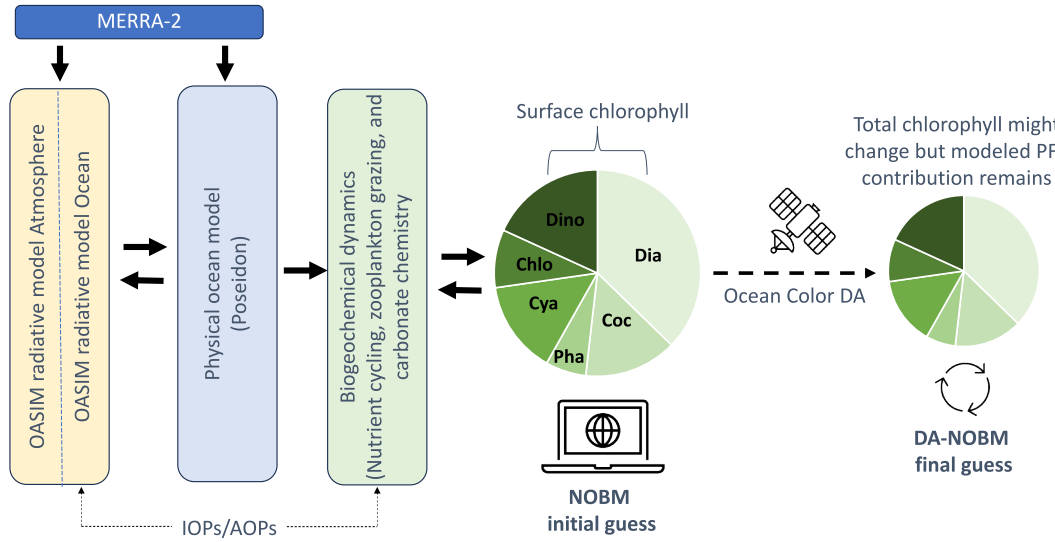

Figure 1. Principal components of the NASA Ocean Biogeochemical Model (NOBM). Climatological output from the Modern-Era Retrospective analysis for Research and Applications version 2 (MERRA-2) is used to force the Ocean-Atmosphere Spectral Irradiance Model (OASIM) and the physical circulation model (Poseidon). Within each grid-cell of the three-dimensional circulation model, sources and sinks of non-conservative biologically-active components (plankton, nutrients, and carbonate-species) are computed by the biogeochemical/ecological module. Biogeochemical components with important light absorption and backscattering properties inform the radiative transfer form for the computation of IOPs and AOPs. The initial estimation (guess) of total phytoplankton chlorophyll biomass is obtained from the sum of the individual chlorophyll concentration of six phytoplankton group: diatoms (Dia), coccolithophores (Coc), chlorophytes (Chlo), dinoflagellates (Dino), cyanobacteria (Cya), and phaeocystis (Pha). The final model estimate is obtained after the data assimilation (DA) of satellite ocean color to achieve improved surface chlorophyll fields.

obtained from the Ocean-Atmosphere Spectral Irradiance Model (OASIM) (Gregg & Casey, 2009), which simulates the propagation of downward spectral irradiance in the atmosphere and ocean, and accounts for the relationship between inherent and apparent optical properties (IOP's and AOP'S) for the calculation of remote sensing variables in the surface ocean. Both OASIM and Poseidon components are forced by the Modern-Era Retrospective analysis for Research and Applications version 2 (MERRA-2) (Gelaro et al., 2017; Rienecker et al., 2011) which includes information on wind speed and stress, sea surface temperature, shortwave radiation, relative humidity, sea level pressure, sea ice fraction, cloud fraction and optical thickness (Figure 1).

The NOBM presently assimilates three distinct remote sensing variables, including chlorophyll, particulate inorganic carbon (PIC), and absorption by colored dissolved organic matter (aCDOM). The type of forward or sequential DA employed operates directly on the model outputs, which are driven toward (satellite) observations through constant confrontation with data (Gregg, 2008). Sequential DA methods are unable to conserve mass but tend to have lower computational costs than inverse modeling methods. An initial guess of total chlorophyll biomass is computed in the model by inferring first the individual biomass of its six phytoplankton functional types. The added chlorophyll biomass of the six PFTs (i) yields the total chlorophyll concentration ($\mathrm{Chl}_{\mathrm{tot}}$) at each model grid box.

$$\mathrm{Chl}_{\mathrm{tot}} = \sum_{n=1}^{6} \mathrm{Chl}_{(i)} \quad (1)$$

$\mathrm{Chl}_{\mathrm{tot}}$ is adjusted based on satellite information but the relative contribution of each PFT to total chlorophyll biomass is determined by the internal biogeochemical component of the model and preserved through the assimilation step (Figure 1). The adjustment of $\mathrm{Chl}_{\mathrm{tot}}$ involves altering the model chlorophyll field to match the laplacian of the satellite-based chlorophyll field using the Conditional Relaxation Analysis Method (CRAM, Oort, 1983; Gregg, 2008), and occurs only at the uppermost layer of the model, which represents the surface mixed layer. DA does not directly alter the remeinder 13 vertical layers of the model, but the depth-structure in chlorophyll can be affected by the adjustment in surface fields.

10.1029/2023EA003378

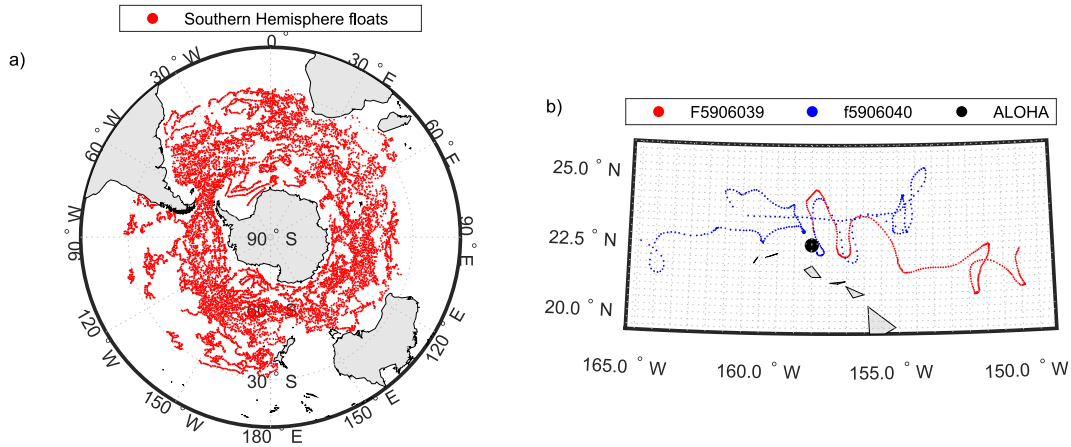

Figure 2. Trajectories of BGC-Argo floats used in this study. (a) Southern Hemisphere float trajectories. (b) Trajectories of floats nearby station ALOHA used for the comparison of float and model profiles against in situ data.

The fields assessed in this study are derived from a model simulation that was initially spun up in free-run mode for 200 years using climatological forcing from MERRA (Rienecker et al., 2011). Starting in 1980, the model is forced with monthly MERRA-2 data, and began assimilating satellite ocean color data from SeaWiFS (9 km) in January 1998. Output from this last step is used to initialize the assimilation of MODIS (9 km) ocean color retrievals in July 2002. Daily output from the MODIS-assimilated run between July 2002 and December 2020 is analyzed in this study.

2.2. BGC-Argo Data

Float data was obtained from the SOCCOM quarterly snapshot archive (https://soccompu.princeton.edu/www/index.html), which includes profiling data from the SOCCOM and GO-BGC programs. Specifically, we obtained the latest low-resolution data snapshot in MATLAB format, published with date 21 December 2022 (Riser et al., 2023). Profiles are available from 27/Mar/2014 (earliest profile) until the publication date, including information from an array of 225 floats and 25,182 profiles (Figure S1 in Supporting Information S1). We use the SOCCOM/GO-BGC data set given that all bio-optical profiles are treated in a consistent and documented manner, which is important given the uncertainty in fluorescence-based float chlorophyll estimates (see below). Most of the data pertains to the Southern Hemisphere, particularly the Southern Ocean (south of 30°S) (Figure 2a). In order to compare both float and model profiles with available in situ data, we also assess profiling information from floats F5906039 and F5906040 (WMO#) near station ALOHA (Figure 2b). Float sampling takes place every 5 m in the upper 100 m, with the uppermost sampled depth ~5 or 7 m below surface. The vertical sampling resolution decreases to 10 m below 100 m depth, 20 m below 360 m depth, and 50 m between 400 and 2,000 m depth. Vertical profiles of float data are interpolated to a 1 m resolution and smoothed using a seven point running-median filter (Arteaga et al., 2020; Boss & Behrenfeld, 2010). SOCCOM floats sample the vertical water column every 5 or 10 days, depending on the preset programming of the float, with most floats sampling every 10 days. Float data with a QC-flag other than "good" (i.e., QC-flag $\neq 0$) were converted to NaNs. Float chlorophyll estimates are based on fluorescence excitation at 470 nm, which involves both chlorophyll-a and accessory pigments, while the emission wavelength is at 695 nm, with a volume measurement of 3 ml (Johnson et al., 2017).

A correction factor of $\frac{1}{2}$ is applied to all chlorophyll profiles in the downloaded data set, which is based on the global average relationship between fluorescence and chlorophyll concentration (Roesler et al., 2017). However, analyses of Southern Ocean float bio-optical data suggest that a stronger slope correction for the conversion between fluorescence and chlorophyll might be required for profiles in this region due to the effects of iron limitation on phytoplankton physiology (Schallenberg et al., 2022). An initial comparison based on 2166 bio-optical profiles obtained from a subset of 56 SOCCOM floats (deployed before March 2016) indicated that a correction factor of 6 yielded the best linear fit to high-performance liquid chromatography (HPLC) pigment measurements collected during float deployments (Johnson et al., 2017). A single correction factor for the entire

Southern Ocean might not be completely adequate since other regional analyses have found a range of variability from ~3 to 8, with more recent studies, aided by a higher density of data, suggesting a correction factor near 4 (Schallenberg et al., 2022). In addition to nutrient limitation, community and relative pigment composition, cell size, and photoacclimation status can alter the relationship between fluorescence and chlorophyll-a (Cullen, 1982; Greg Mitchell & Kiefer, 1988; Proctor & Roesler, 2010). Given these recent findings but still overall regional uncertainty around this factor, we have removed the original correction of $\frac{1}{2}$ and applied a new correction of $\frac{1}{4}$ to all float profiles south of 30°S.

2.3. ALOHA Data

Float and model data are compared against depth-resolved chlorophyll profiles at station ALOHA, part of the Hawaii Ocean Time-series (HOT) program, and located at 22° 45′N, 158°W (Figure 2b). These data are obtained from seawater samples collected using a CTD-rosette, where photosynthetic pigments are extracted from sub-samples filtered onto glass fiber filters and placed into cold, 100% acetone. The concentration of chlorophyll and other pigments are measured by fluorometry (see details on the analytical sampling method at https://hahana.soest.hawaii.edu/hot/protocols/protocols.html). In situ data included in this study span from 1988 to 2021. Data were obtained via the Hawaii Ocean Time-series HOT-DOGS application (http://hahana.soest.hawaii.edu/hot/hot-dogs/).

3. Analyses and Data Subsampling

3.1. General Model-Float Comparison

We subsampled the quasi-lagrangian float trajectories within the model by obtaining daily NOBM chlorophyll profiles at the same date and nearest grid location to that of our float-based profiles. Given that the time span of our model simulation and float data set do not fully overlap, our model-float daily matching effectively encompassed the period between the earliest float profile (27/Mar/2014) and latest NOBM daily output (31/Dec/2020). We begin by examining the surface mixed layer daily output from the model and BGC-Argo floats (Figure 3). For each daily matchup, we adapt the higher vertical resolution of the floats to the coarser depth resolution of the model: The uppermost chlorophyll value of the model is compared against the median float chlorophyll concentration over the mixed layer predicted by the model. For each model vertical layer below the mixed layer, the median float chlorophyll concentration between the upper and lower vertical boundaries of the model is compared against the model's chlorophyll concentration at that layer. Thus, resulting float-based depth profiles have 14 vertical values that match the model vertical coordinates. Following the evaluation of surface fields, we compare the frequency distribution in chlorophyll concentration at various depths (Figure 4) and overall model-float data missfit along the water column (Figure 5).

3.2. Seasonal Comparison at ALOHA

We compare model and float profiles against depth-resolved in situ observations from station ALOHA. Individual and seasonally-averaged float and model data are compared against in situ profiles for Winter (January–March), Spring (April–June), Summer (July–September), and Fall (October–December) (Figure 6). BGC-Argo data (and corresponding model output) includes only profiles from floats F5906039 and F5906040 (Figure 2b). For this local comparison all three data sources (model, float, and in situ) are vertically-binned by averaging chlorophyll profiles in 10 m depth-intervals between surface and 200 m. Binned float data consisted of original downloaded profiles with high vertical resolution. Note that depth coordinates in the NOBM are not static, thus, model chlorophyll information at certain depths and seasons can be missing.

3.3. Binned Southern Ocean Seasonal and Meridional Model-Float Comparison

We computed monthly- and zonally-averaged depth-profiles of float and model matching profiles produced in Section 3.1 (i.e., model profiles were obtained based on the float's date and location, while matching float profiles were subsampled according to the model's 14-layers depth coordinates). For monthly averages, profiles were divided in 10° meridional bins from 20°S to 80°S (Figure 7). Since the model vertical coordinates are not static, model and float profiles are averaged monthly and by 10 m depth-intervals between surface and 200 m. Vertical profiles of model-float differences were sorted and averaged in the same manner. (Figure 8). For zonal averages, profiles were divided for the Atlantic, Indian and Pacific basins of the Southern Ocean (Figures 9 and 10). Profiles

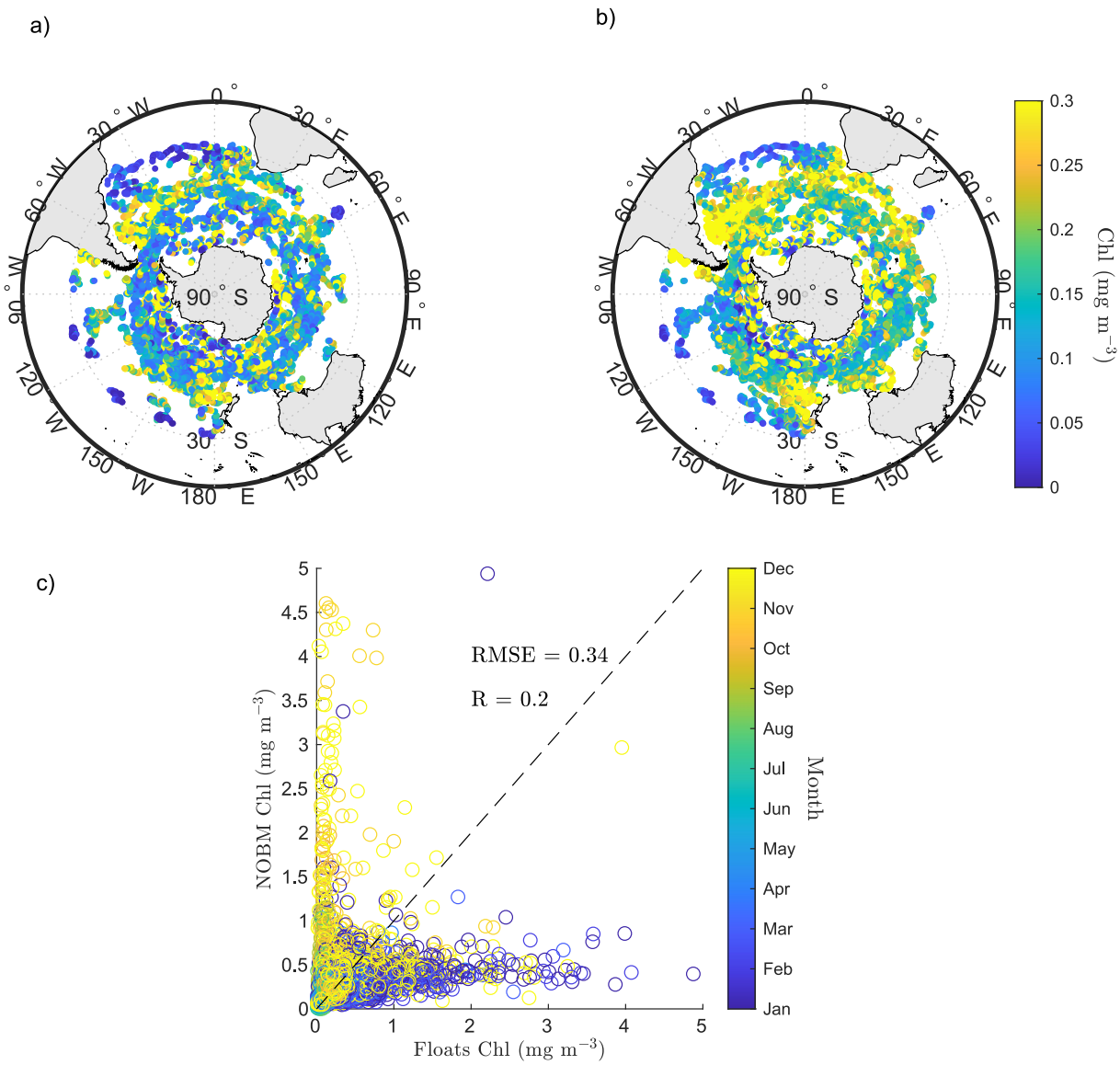

Figure 3. Surface mixed layer chlorophyll (Chl) concentration inferred from (a) BGC-Argo floats and (b) matching NOBM output in the Southern Ocean. (c) Scatterplot of surface Chl concentration from floats and the NOBM. Colors indicate the corresponding month of each float/model output. The dashed-black line represents the 1:1 relationship between model and float estimates.

were sorted in 5° meridional bins from 20°S to 75°S and averaged in 10 m depth-intervals between surface and 200 m. Our model subsampling of matching float profiles assigns NaNs to model profiles when the entire corresponding float profile is missing information or values were flagged ≠0 during the quality-control process (white areas in climatological Southern Ocean profiles, Figures 7–10).

4. Results and Discussion

4.1. General Surface and Depth Patterns in Model and Float Chlorophyll Estimates

Modeled surface mixed layer patterns in Southern Ocean chlorophyll concentration show a similar spatial distribution to that inferred from floats (Figure 3), with highest values off the Argentinian Patagonian coast and around the circumpolar ring centered at 50°S, where nutrient-rich water is upwelled south of the Polar Front (Marinov et al., 2006; Sarmiento et al., 2004). However, modeled fields overestimate float estimates in regions of high chlorophyll concentration. Overall, modeled mixed layer chlorophyll is higher than float estimates during the

10.1029/2023EA003378

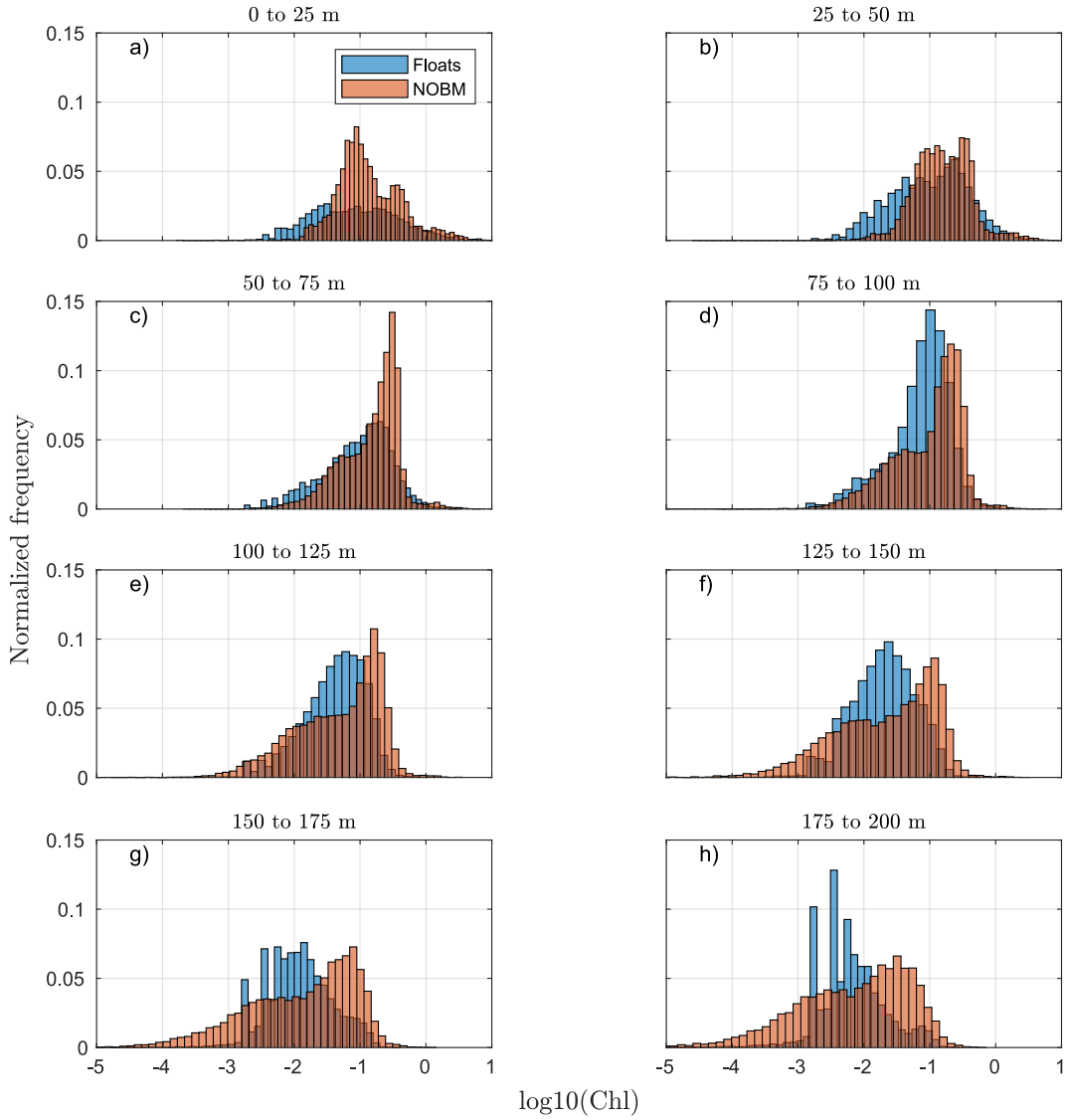

Figure 4. Normalized frequency histograms of chlorophyll (Chl) (mg m^{-3}) concentration from BGC-Argo floats (blue bars) and NOBM (orange bars) estimates obtained over various depth ranges: (a) 0–25 m, (b) 25–50 m, (c) 50–75 m, (d) 75–100 m, (e) 100–125 m, (f) 125–150 m, (g) 150–175 m, (h) 175–200 m.

highly productive austral spring months (October–December), and lower during the less productive fall–winter season (Figure 3c). This general pattern of higher modeled estimates (with respect to floats) at high chlorophyll levels, and vice versa, can also be inferred from the normalized frequency distribution of model and float chlorophyll concentration at various depth ranges (Figure 4). Model and float chlorophyll values between 0 and 25 m and 25–50 m show a log-normal (base-10) distribution, with a higher model frequency in the 10^{-2} to 10^{0} (mg Chl m^{-3}) range, and higher float frequency for concentrations $<10^{-2}$ mg Chl m^{-3} (Figures 4a and 4b). In the 50–75 m and 75–100 m, the high-value tail of the distribution is lower than in the surface layers, with most values constrained to $<10^{0}$ mg Chl m^{-3}. Both model and float estimates show a distribution slightly biased toward higher values (within this range) between 10^{-1} and 10^{0} (mg Chl m^{-3}), with model concentrations showing slightly higher frequency than floats in the higher range of values between 50 and 100 m (Figures 4c and 4d). Deeper in the water column (between 100 and 200 m), both model and floats show overall lower chlorophyll concentrations than at shallower depths, and a starker divergence in output frequency, where model output is more recurrent toward the tails of the distributions ($<10^{-3}$ and $>10^{-1}$ mg Chl m^{-3}), while float values are more prevalent in the 10^{-3} to 10^{-1} (mg Chl m^{-3}) range (Figures 4e–4h).

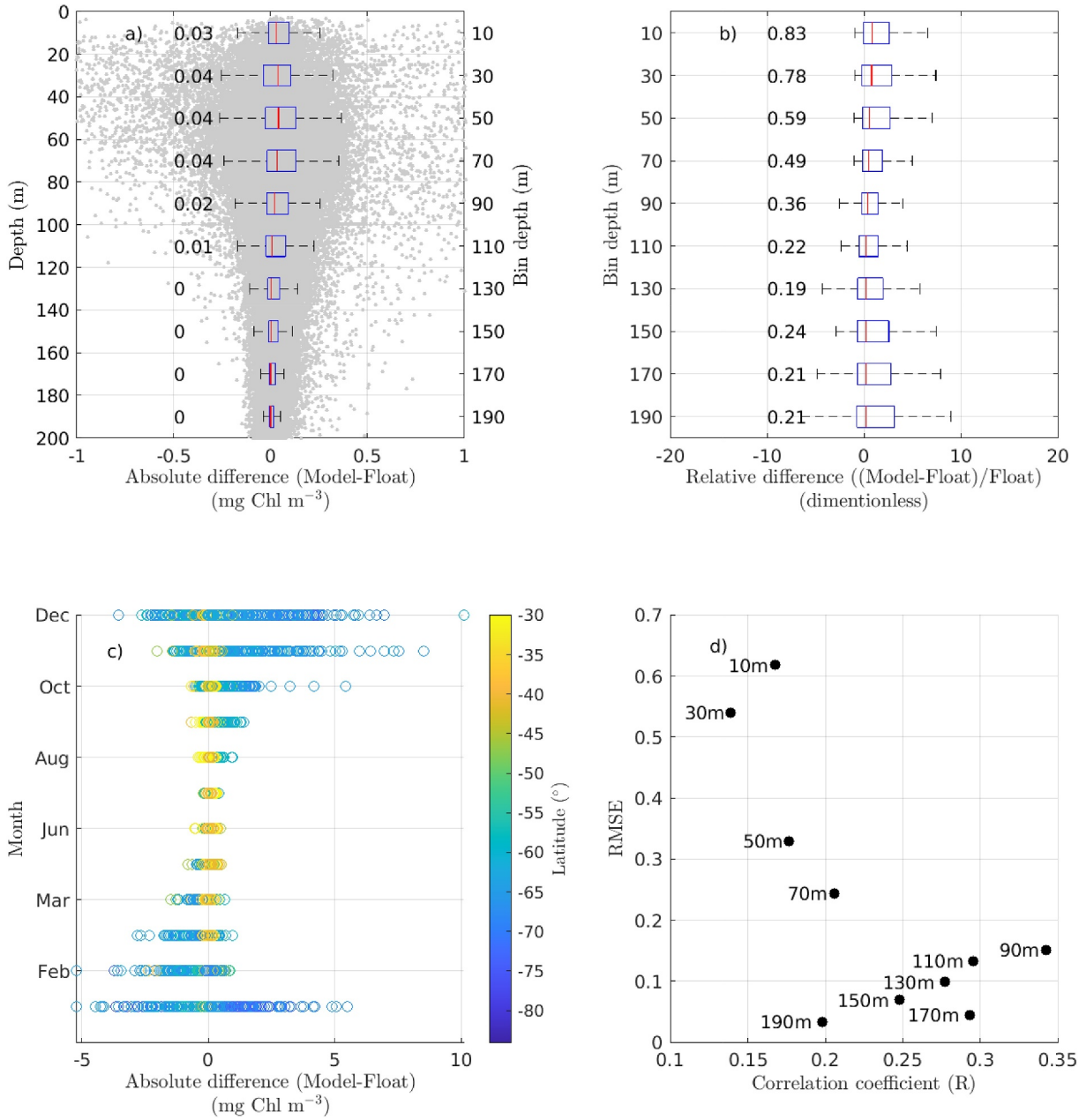

Figure 5. (a) Absolute difference between individual BGC-Argo and NOBM chlorophyll (Chl) estimates at different depths. Differences are computed based on float profiles adapted to the model vertical coordinates. Box and whisker plots of model-floats differences are obtained for 20 m depth bins between surface and 200 m. The red line of the box plot indicates the median value of the sample, while the blue edges of the box indicate the 25th and 75th percentile. The whiskers extend to the most extreme data points not considered outliers. The center depth of each bin is indicated on the right *Y*-axis. (b) Box plots of relative difference (normalized by float value) between model and floats Chl estimates. Depth bins are obtained similarly as in panel (a). (c) Relationship between the absolute difference in model-float Chl estimates and the corresponding month and latitude of the model/float estimate. (d) Scatterplot of the Root-Mean-Square Error (RMSE) and correlation coefficient (*R*) between float and model Chl estimates obtained over 20 m depth bins between surface and 200 m. Depth levels indicate the center of the depth bin.

4.2. Model-Floats Vertical Missfit in Chlorophyll

As it can be inferred from Section 4.1, model chlorophyll output overestimates float chlorophyll on average throughout the water column (Figure 5a). For model-float differences sorted in 20 m depth bins between surface and 200 m, the largest median model-float missfit is of 0.04 mg Chl m^{-3}, obtained for bin-layers centered at 30, 50, and 70 m. The median model-float missfit is of 0.03 mg Chl m^{-3} within the upper 20 m, and decreases to negligible values below 110 m. The 25th and 75th percentiles edges of difference in chlorophyll concentration

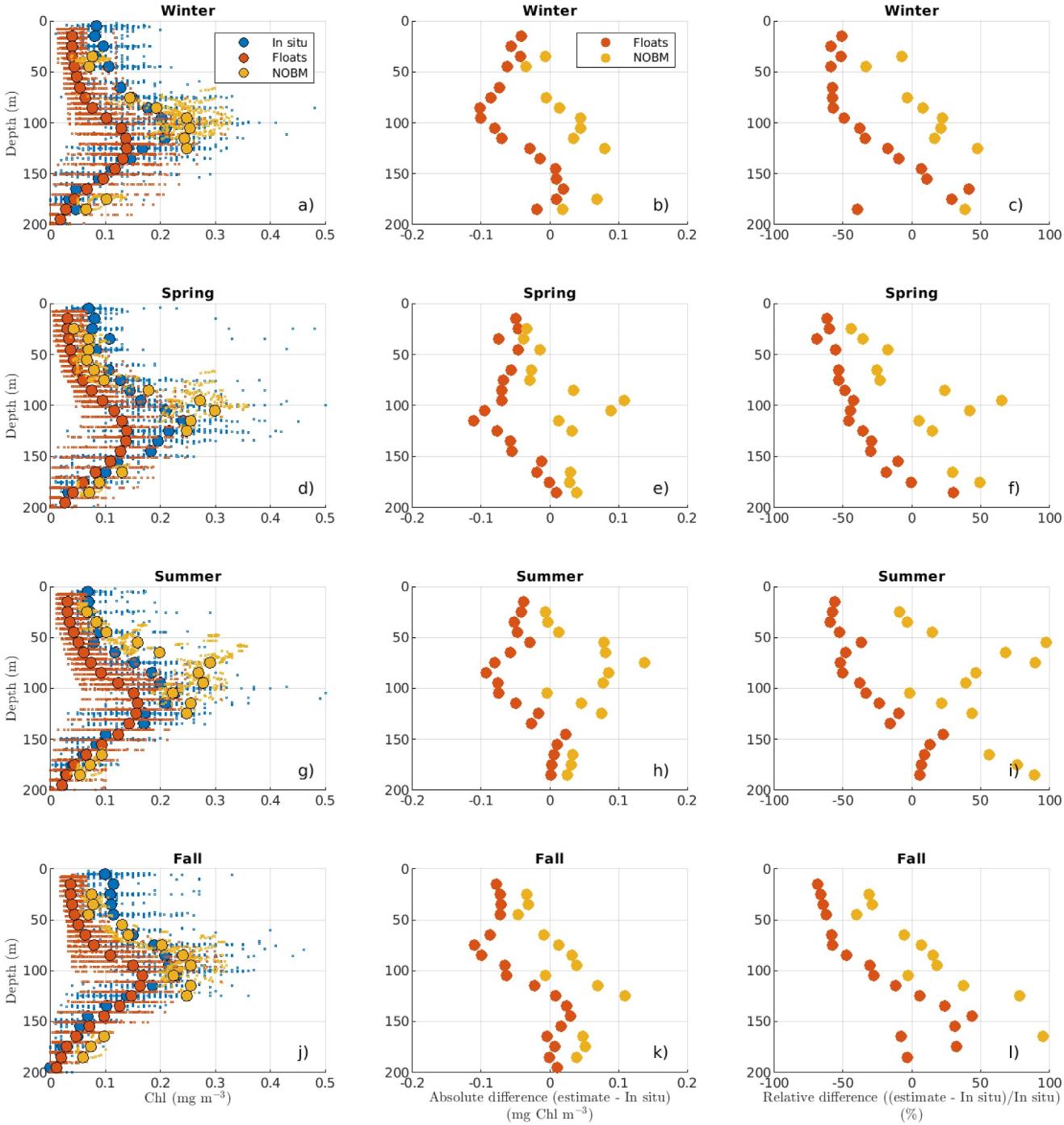

Figure 6. Vertical chlorophyll (Chl) profiles from BGC-Argo floats (red), NOBM (yellow), and in situ data (blue) at station ALOHA. Left panels (a), (d), (g), and (j) show Chl concentration from individual profiles (small circles) and seasonally- and depth-averaged data (large circles). Center panels (b), (e), (h), and (k) show absolute differences between averaged float and model estimates with respect to in situ measurements. Right panels (c), (f), (i), and (l) show relative differences (normalized by in situ measurements) between averaged float and model estimates with respect to in situ measurements.

binned across depths are constrained within ±0.25 mg Chl m^{-3}, but non-outlier extremes can approach ±0.5 mg Chl m^{-3}. The float-normalized median relative difference between model and float chlorophyll is about 0.8 (80%) in the upper 20 m and decreases with depth to ~0.2 (20%) between 160 and 200 m (Figure 5b). While the median relative bias declines with the depth, its overall range increases to nearly ±10 (1,000%), as the signal-to-noise ratio for accurate float chlorophyll estimation by the model declines sharply with depth.

10.1029/2023EA003378

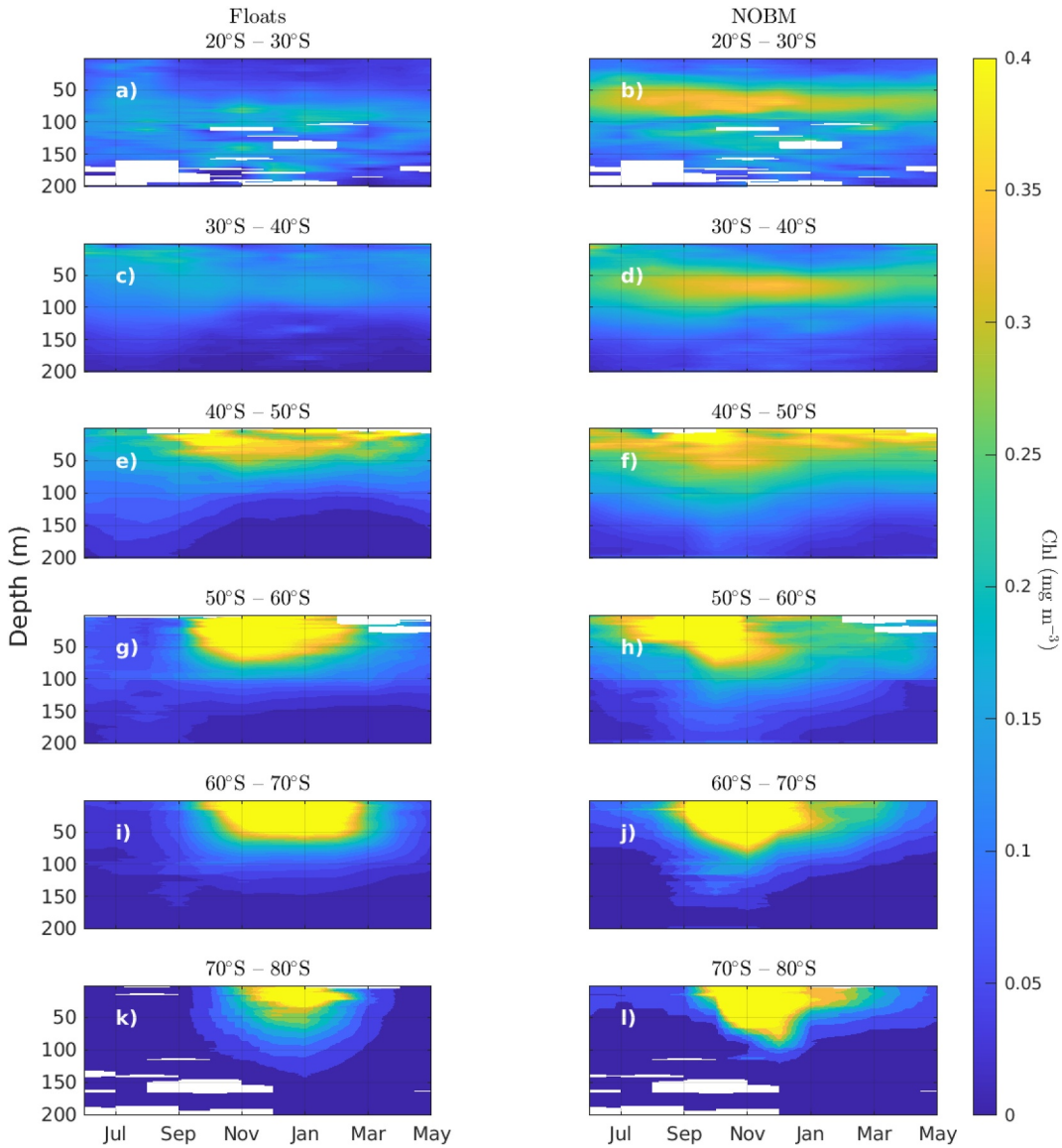

Figure 7. Monthly- and depth-averaged chlorophyll (Chl) profiles from BGC-Argo floats (left panels) and the NOBM (right panels). Profiles are divided in 10° meridional bins: 20°S–30°S (a) and (b), 30°S–40°S (c)–(d), 40°S–50°S (e) and (f), 50°S–60°S (g) and (h), 60°S–70°S (i) and (j), and 70°S–80°S (k) and (l).

The largest differences between model and float chlorophyll at all depths are observed during late spring (November–January) and for regions south of 60°S (Figure 5c). It is important to note that model-float differences are sensitive to the correction factor applied to float fluorescence profiles to estimate chlorophyll in the Southern Ocean (Section 2.2). A sensitivity analysis performed with a randomly selected subset of floats (25% of the entire array), showed that the original Southern Ocean SOCCOM correction factor of $\frac{1}{2}$ results in reduced overestimation, or even underestimation, of the float data by the model chlorophyll fields at some depths, while a correction factor of $\frac{1}{6}$ (suggested by earlier SOCCOM studies, Johnson et al., 2017) or $\frac{1}{8}$, yield a yet larger overestimation of float chlorophyll by the model (Figure S2 in Supporting Information S1). The characterization of model-float data missfit with depth provides an intuition for the general bias in modeled chlorophyll by the NOBM with respect to the BGC-Argo data array, but underestimates the overall model error in predicting float profiles (by combining and canceling positive with negative deviations) (Figures 5a–5c). The Root-Mean-Square Error (RMSE) between model and float data is highest for chlorophyll estimates in the upper 20 m (depth bin centered at 10 m, RMSE ~ 0.6 mg Chl m^{-3}), and decreases monotonically with depth (Figure 5d). Given that the dynamic range in

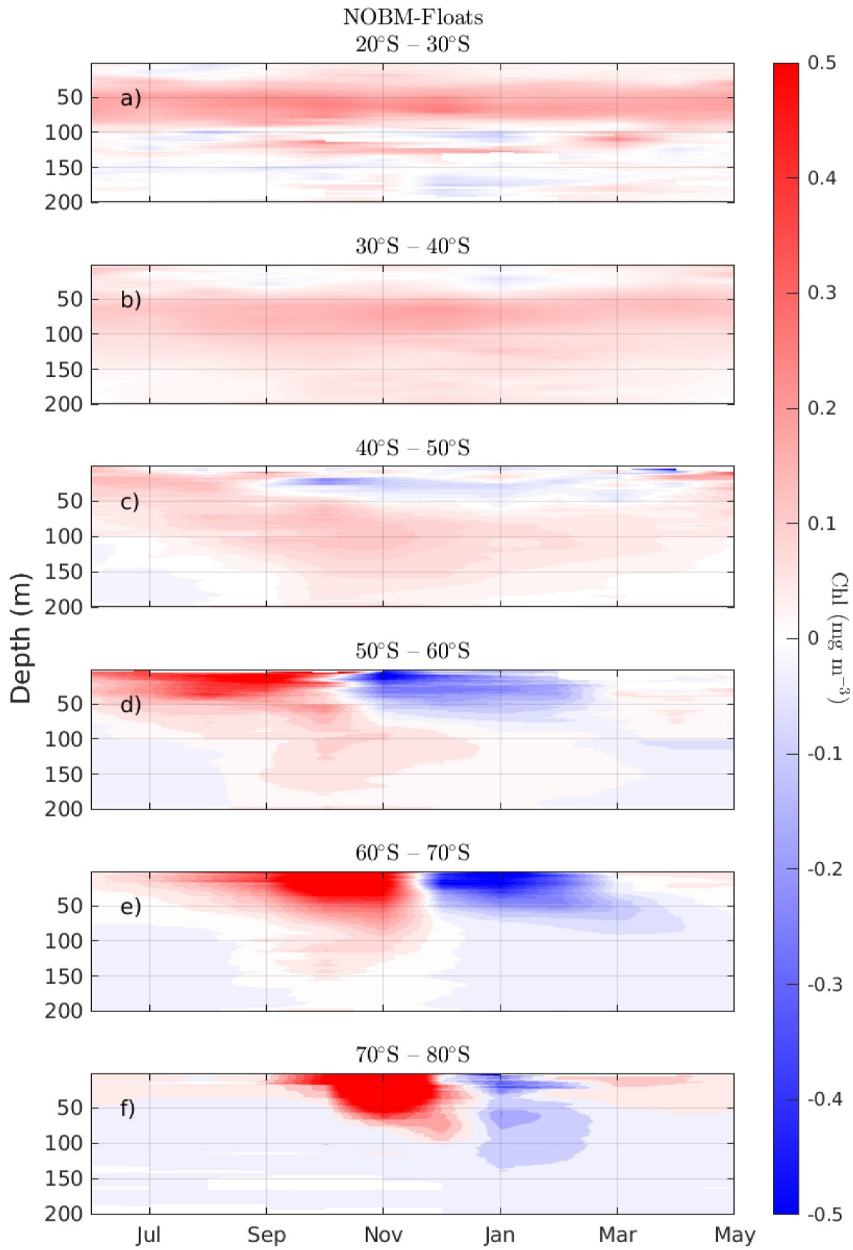

Figure 8. Monthly- and depth-averaged difference between NOBM and BGC-Argo float chlorophyll (Chl) profiles. Profiles are divided in 10° meridional bins: 20°S–30°S (a), 30°S–40°S (b), 40°S–50°S (c), 50°S–60°S (d), 60°S–70°S (e), and 70°S–80°S (f).

float chlorophyll spans over three orders of magnitude, roughly between 0.01 and >1 mg Chl m^{-3} (Figure 4), a model error between 0.1 and 0.6 mg Chl m^{-3} should allow the detection of seasonal changes in float-based biomass, but likely hinders the detection of subtle changes in chlorophyll at narrow local scales.

The correlation coefficient (R) between model and float chlorophyll concentration within each depth bin is always positive and varies between 0.1 and 0.35, indicating that the model likely describes some of the main mechanistic drivers of chlorophyll variability, but fails to represent the full variance of the float array. The lowest correlation is observed for the uppermost depth bins at 10, 30, 50 m, with R varying roughly between 0.125 and <0.2. These are the depth layers of the water column where most of the productivity and biogeochemical cycling occurs, and thus, the most challenging depth levels for the model to replicate and resolve over the vertical dimension. The highest correlation coefficient is obtained at around 100 m ($R \sim 0.3$–0.35). At this depth range, any local production of

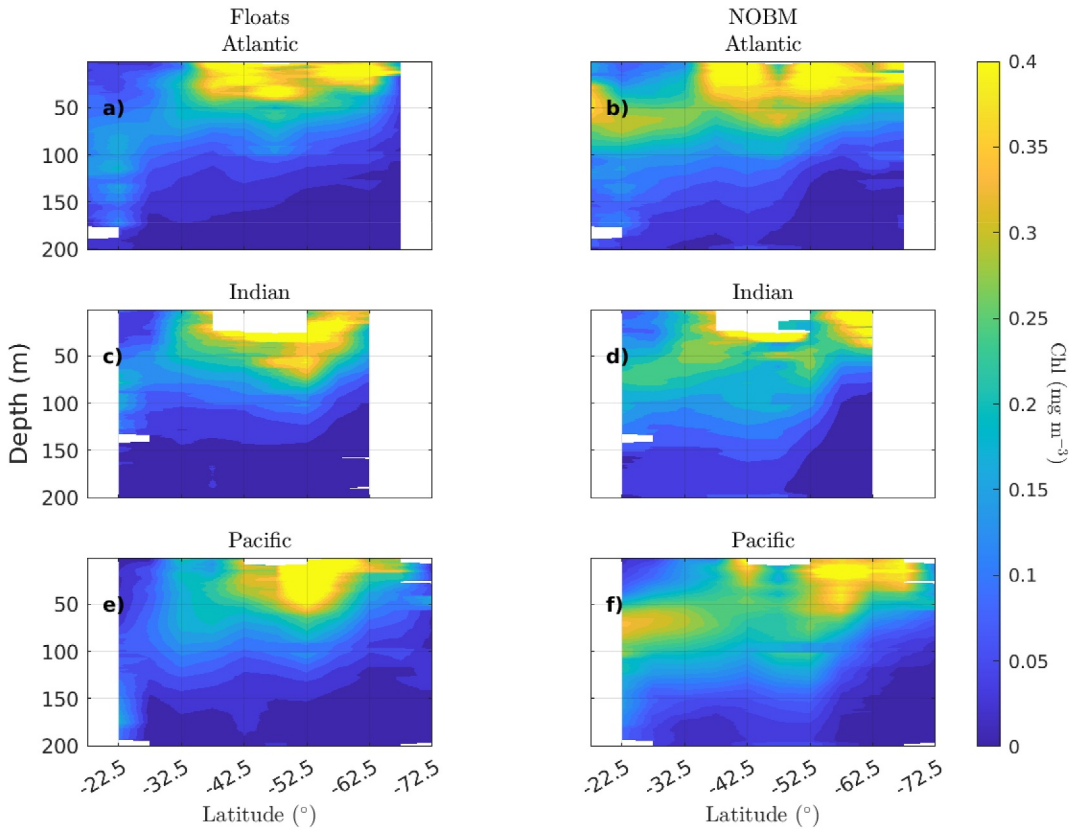

Figure 9. Zonally- and depth-averaged chlorophyll (Chl) profiles from BGC-Argo floats (left panels) and the NOBM (right panels). Profiles are divided into the Atlantic (a) and (b), Indian (c) and (d), and Pacific (e) and (f) basins of the Southern Ocean.

biomass is expected to be less acute than in the upper 50 m, while surface productivity bursts have likely been smoothed out through particle sinking and gradual remineralization, yielding a more stable monthly or seasonal time-scale of variability in chlorophyll biomass. Below 100 m, the signal-to-noise ratio in modeled chlorophyll decreases rapidly leading to a further overall reduction in correlation with float estimates.

4.3. Seasonal Profiles at ALOHA

Averaged profiles from floats F5906039 and F5906040 and their respective NOBM pairings replicate generally well the mean vertical structure of in situ chlorophyll profiles at station ALOHA (Figure 6). The correlation coefficient (R) between mean modeled and in situ profiles is above 0.8 for all seasons, and slightly lower, but also positive and relatively high (>0.7), between BGC-Argo floats and in situ observations (Table 1). The root mean square error (RMSE) between mean model and in situ profiles varies between 0.03 and 0.05 mg Chl m^{-3} and it is lower than the RMSE between floats and in situ profiles in all seasons except fall (ranging between 0.04–0.06 mg Chl m^{-3}, Table 1).

In situ profiles show a deep chlorophyll maximum (DCM) at around 100 m, which is replicated by the model and, less acutely, by the floats (Figure 6). Similarly as with the analysis of bulk data above (dominated by Southern Ocean profiles), modeled chlorophyll tends to be higher than float estimates, specially in the upper 150 m. Across all seasons, in situ chlorophyll profiles are mostly higher than both float- and model-based estimates in the upper 50 m. In the vertical region centered around the DCM (50–150 m), the model overestimates in situ chlorophyll, while floats underestimate it. Over the upper 200 m (where observations are available), the average model bias is positive with respect to in situ measurements (varying between 0.02 and 0.05 mg Chl m^{-3}), while float-based estimates show a larger (except for fall) but negative mean bias across all seasons with respect to in situ profiles (ranging between −0.03 and −0.05 mg Chl m^{-3}) (Table 1). This pattern can also be appreciated in the depth-resolved absolute difference between mean float and model profiles with respect to in situ data (Figure 6, center

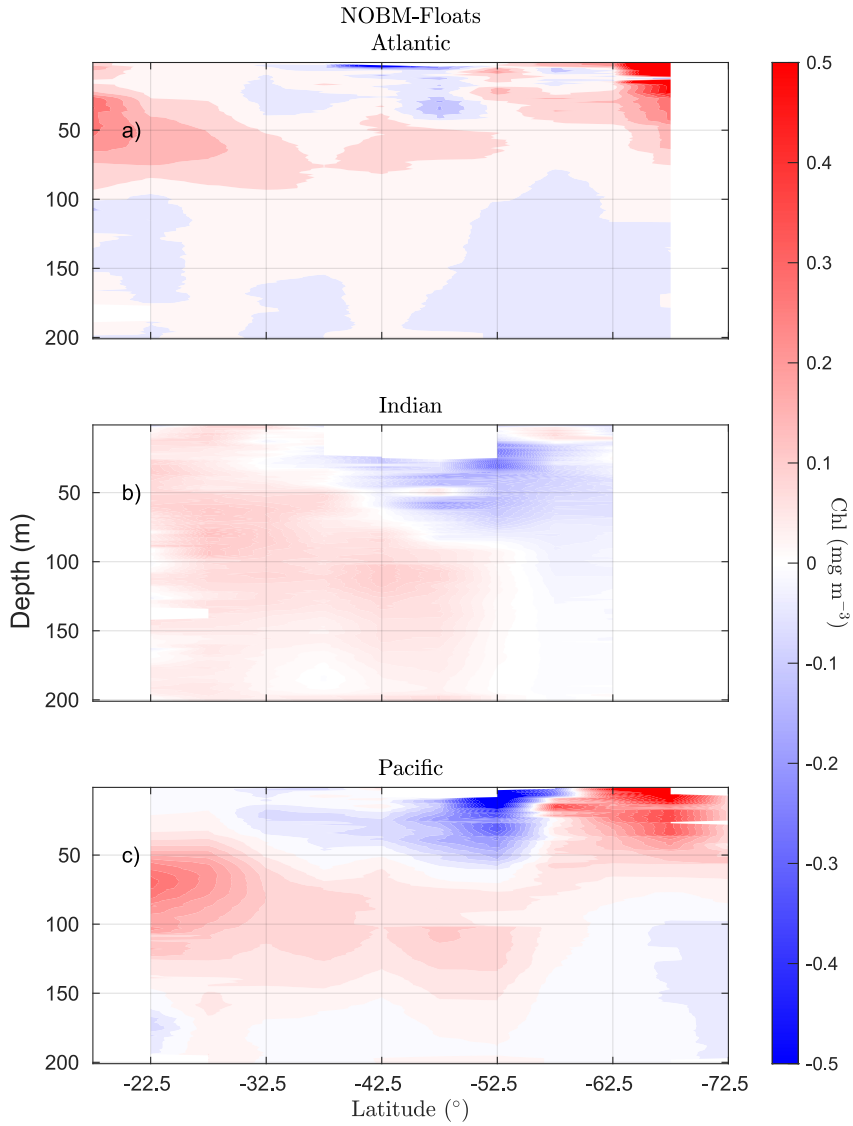

Figure 10. Zonally- and depth-averaged difference between NOBM and BGC-Argo float chlorophyll (Chl) profiles. Profiles are divided into the Atlantic (a), Indian (b), and Pacific (c) basins of the Southern Ocean.

Table 1
Correlation Coefficient (R), Root Mean Square Error (RMSE), and Mean Bias of the Seasonally Averaged Vertical Profiles From BGC-Argo Floats and NOBM Estimates with Respect to Seasonally Averaged Vertical Profiles of In Situ Chlorophyll Data at Station ALOHA (Presented in Figure 6)

	R		RMSE (mg Chl m^{-3})		Bias (mg Chl m^{-3})	
Season	Float	NOBM	Float	NOBM	Float	NOBM
Winter	0.76	0.9	0.05	0.03	−0.04	0.03
Spring	0.89	0.88	0.06	0.04	−0.05	0.02
Summer	0.85	0.89	0.04	0.05	−0.03	0.05
Fall	0.77	0.84	0.05	0.04	−0.03	0.02

panels), which is mostly constrained between ±0.1 mg Chl m^{-3}. In relative terms, most mean float and model depth-resolved estimates are within ±50% of in situ measurements (Figure 6, right panels). Floats slightly underestimate in situ observations by more than (−) 50% across all seasons for depths shallower than 100 m. Model outputs overestimate in situ chlorophyll by more than (+) 50% primarily in summer between 50 and 100 m, and below 150 m, and less frequently below 100 m in Fall.

4.4. Seasonality in Southern Ocean Float and Modeled Chlorophyll Depth-Profiles

Binned modeled and float-based profiles show similar seasonality in chlorophyll concentration across most of the Southern Ocean (Figure 7). Seasonality is reduced in the subtropical sections of the Southern Hemisphere (north of 40°S), with modeled outputs showing a clear DCM between 50 and 100 m (Figures 7b and 7d). BGC-Argo floats also present higher levels of

Table 2
Correlation Coefficient (R), Root Mean Square Error (RMSE), and Mean Bias, Between Binned BGC-Argo Float and NOBM Profiles in the Southern Ocean (Corresponding to Figure 7 (Seasonal Comparison) and Figure 9 (Latitudinal Comparison))

	R	RMSE (mg Chl m^{-3})	Bias (mg Chl m^{-3})
Meridional region (seasonal comparison)			
20°S–30°S	0.5	0.1	0.06
30°S–40°S	0.86	0.08	0.06
40°S–50°S	0.88	0.07	0.04
50°S–60°S	0.65	0.12	0.04
60°S–70°S	0.67	0.16	0.02
70°S–80°S	0.52	0.25	0.05
Basin (latitudinal comparison)			
Atlantic	0.8	0.09	0.06
Indian	0.86	0.06	0.02
Pacific	0.72	0.1	0.04

subsurface chlorophyll with respect to the surface, but their magnitude is much lower than that of the NOBM (Figures 7a and 7c). South of 40°S, both modeled and float data show a tendency of delayed bloom onset and termination with increasing latitude (Figures 7e–7l). The meridional section between 40°S and 50°S (Figures 7e and 7f) has overall lower modeled and float-based chlorophyll concentrations sustained throughout most of the pseudo-climatological year when compared with sections south of 50°S, where the high biomass period is primarily constrained between September and March (Figures 7g–7l). On average, modeled and float profiles are better correlated and show lower discrepancy (assessed via *R* and RMSE, Table 2) in the 30°S to 50°S meridional bins, with correlation decreasing and model error increasing polewards and for the 20°S to 30°S region.

Differences between modeled and float chlorophyll indicate that the model overestimates the float array north of 40°S throughout all seasons (Figures 8a and 8b). South of 40°S, an interesting dynamic emerges, where the NOBM overestimates float chlorophyll during the first phase of the spring bloom and underestimates it during summer and fall months (Figures 8c–8f). The overall missmatch between model and float data is more acute polewards and south of 50°S compared to the more subtropical sections. It is possible that the mechanistic dynamics of the NOBM wrongly trigger the onset of the bloom ahead of what would be observed in situ at higher latitudes. The NOBM is constrained by ocean color satellite observations which should minimize any temporal gap in the "greening" of the surface ocean (as observed from space) and related ecological bloom dynamics, but remote sensing data in the Southern Ocean is hindered by enhanced cloudy conditions and periods of high solar zenith angle over this region (Gregg & Casey, 2007b). Another potential source of disagreement could be temporal changes in the fluorescence-biomass relationship in phytoplankton chlorophyll that are currently not accounted by the fixed correction factor applied to float bio-optical profiles. Comparing modeled phytoplankton carbon against profiles derived from float backscattering sensors might help disentangle some of these processes. Our current NOBM version estimates cellular carbon internally based on a dynamic Chl:C ratio that varies as a function of the environmental light level (Gregg & Casey, 2007a). Unfortunately, Chl:C is presently not saved as part of the biogeochemical suite of model variables, which impedes the offline computation of phytoplankton carbon, but future work is planned to update the model code and surpass this limitation.

4.5. Meridional Patterns in Southern Ocean Float and Modeled Chlorophyll Depth-Profiles

Zonally-averaged binned model and float profiles display similar meridional patterns in all three Southern Hemisphere basins (Atlantic, Indian, and Pacific) (Figure 9). In the Atlantic basin, both modeled and float data show highest surface chlorophyll south of 40°S, while chlorophyll concentration is higher in the subsurface (at or below 50 m depth) toward the equator, indicating the presence of subtropical DCMs, which are more pronounced in the NOBM (Figures 9a and 9b). The Indian and Pacific basins show a similar structure of high subsurface chlorophyll concentration north of 40°S (more accentuated in the NOBM), and higher surface concentrations polewards (Figures 9c–9f). This pattern is consistent with oligotrophic subtropical conditions that yield lesser surface phytoplankton biomass concentration, thereby reducing light attenuation through the water column and permitting the formation of DCMs (Cullen, 2015). At the same time, higher surface chlorophyll concentrations toward the polar front are consistent with the enhanced upwelling of nutrient-rich deep water near this region (Marinov et al., 2006; Sarmiento et al., 2004) (also observed in the surface data depicted in Section 4.1). Differences in inferred modeled and float chlorophyll in the Atlantic and Pacific basins show that the NOBM overestimates float subsurface chlorophyll concentrations, particularly in the 50–100 m depth range (Figures 10a and 10c), which is consistent with what observed in the seasonally binned data of subtropical regions (Figure 7). The NOBM overestimates float chlorophyll near the pole in these two basins, while float data is higher than model estimates in the surface layers between the subtropical and polar fronts (~40°S–50°S), where low iron concentrations limit phytoplankton growth and potentially cellular acclimation to low light conditions (photoacclimation) (Arteaga et al., 2019, 2022; Boyd et al., 2007; Martin et al., 1990). Overall, modeled chlorophyll agrees best with float data in the Indian Ocean (highest *R* and lowest RMSE and bias), followed the Atlantic, and Pacific basins (Table 2).

5. Conclusions

We describe how vertical chlorophyll profiles from the NOBM compare against data from a wide array of BGC-Argo floats primarily deployed in the Southern Ocean, as well as float and in situ profiles around station ALOHA. The model replicates well the general seasonality and meridional gradients in surface and depth-resolved chlorophyll-a inferred from the float array. The median difference in chlorophyll concentration between the model and the float array is +0.03 mg Chl m^{-3} in the upper 20 m and +0.04 mg Chl m^{-3} between 20 and 80 m depth (model high). The NOBM tends to overestimate the float array at times and locations of high productivity such as the beginning of the spring bloom, subsurface layers in the subtropics (DCMs), surface waters off the Patagonian coast, and non iron-limited regions of the Southern Ocean. At station ALOHA, both model and float profiles replicate well the general vertical structure of in situ chlorophyll profiles, which vary on average between 0 and 0.3 mg Chl m^{-3} and show a clear DCM signature between 50 and 100 m. Overall, mean chlorophyll profiles from the NOBM tend to be in better agreement with in situ data (roughly ±50%) than float-based estimates. Uncertainties in fluorescence-based float chlorophyll estimates need to be resolved in order to use BGC-Argo bio-optical data as a reliable benchmark for validation purposes. However, the general qualitative agreement between data from the float array and the NOBM provides confidence in the ability of model to replicate realistic biogeochemical features below the surface, where data is not directly constrained by the assimilation of satellite ocean color. On going and future work includes updating the NOBM code to retrieve offline estimates of Chl:C ratio and conduct similar evaluations on phytoplankton carbon and associated fluxes, as well as coupling the biogeochemical model with a physical circulation model capable of resolving finer spatial scales (i.e., Modular Ocean Model version 5 and 6) as part of NASA's Goddard Earth Observing System (GEOS) models.

Data Availability Statement

Access to output from the NOBM can be gained via https://gmao.gsfc.nasa.gov/reanalysis/MERRA-NOBM/, and code can be accessed via https://gmao.gsfc.nasa.gov/reanalysis/MERRA-NOBM/software/. The MERRA-2 reanalysis data used in this study have been provided by the Global Modeling and Assimilation Office (GMAO) at NASA Goddard Space Flight Center (GSFC), and can be accessed via https://gmao.gsfc.nasa.gov/reanalysis/MERRA-2/data_access/. Assimilated satellite ocean color data can be obtained from the NASA GSFC ocean color web site at https://oceancolor.gsfc.nasa.gov/. The SOCCOM BGC-Argo data used was the low-resolution data snapshot in MATLAB format, published with date 21 December 2022 (Riser et al., 2023), and obtained from the quarterly snapshot archive (https://soccompu.princeton.edu/www/index.html). Data for station ALOHA was obtained via the Hawaii Ocean Time-series HOT-DOGS application (http://hahana.soest.hawaii.edu/hot/hot-dogs/); University of Hawai'i at Mãnoa.

Acknowledgments
We thank the NASA Ocean Ecology Laboratory for providing the satellite ocean color data and the NASA Center for Climate Simulation for computational support. This paper was funded by the NASA Carbon Monitoring System Program (80NSSC23K1231, Principal Investigator: Lionel A. Arteaga).

References

Arteaga, L. A., Behrenfeld, M. J., Boss, E., & Westberry, T. K. (2022). Vertical structure in phytoplankton growth and productivity inferred from biogeochemical-argo floats and the carbon-based productivity model. *Global Biogeochemical Cycles*, *36*(8), e2022GB007389. https://doi.org/10.1029/2022GB007389

Arteaga, L. A., Boss, E., Behrenfeld, M. J., Westberry, T. K., & Sarmiento, J. L. (2020). Seasonal modulation of phytoplankton biomass in the Southern Ocean. *Nature Communications*, *11*(1), 5364. https://doi.org/10.1038/s41467-020-19157-2

Arteaga, L. A., Pahlow, M., Bushinsky, S. M., & Sarmiento, J. L. (2019). Nutrient controls on export production in the Southern Ocean. *Global Biogeochemical Cycles*, *33*(8), 942–956. https://doi.org/10.1029/2019GB006236

Arteaga, L. A., & Rousseaux, C. S. (2023). Impact of Pacific Ocean heatwaves on phytoplankton community composition. *Communications Biology*, *6*(263), 263. https://doi.org/10.1038/s42003-023-04645-0

Behrenfeld, M. J., & Falkowski, P. G. (1997). A consumer's guide to phytoplankton primary productivity models. *Limnology & Oceanography*, *42*(7), 1479–1491. https://doi.org/10.4319/lo.1997.42.7.1479

Boss, E., & Behrenfeld, M. (2010). In situ evaluation of the initiation of the North Atlantic phytoplankton bloom. *Geophysical Research Letters*, *37*(18), L18603. https://doi.org/10.1029/2010GL044174

Boyd, P. W., Jickells, T., Law, C. S., Blain, S., Boyle, E. a., Buesseler, K. O., et al. (2007). Mesoscale iron enrichment experiments 1993-2005: Synthesis and future directions. *Science*, *315*(5812), 612–617. https://doi.org/10.1126/science.1131669

Carr, M., Friedrichs, M., Schmeltz, M., Noguchiaita, M., Antoine, D., Arrigo, K., et al. (2006). A comparison of global estimates of marine primary production from ocean color. *Deep Sea Research Part II: Topical Studies in Oceanography*, *53*(5–7), 741–770. https://doi.org/10.1016/j.dsr2.2006.01.028

Chai, F., Johnson, K. S., Claustre, H., Xing, X., Wang, Y., Boss, E., et al. (2020). Monitoring ocean biogeochemistry with autonomous platforms. *Nature Reviews Earth & Environment*, *1*(6), 315–326. https://doi.org/10.1038/s43017-020-0053-y

Claustre, H., Johnson, K. S., & Takeshita, Y. (2020). Observing the global ocean with biogeochemical-argo. *Annual Review of Marine Science*, *12*(1), 23–48. https://doi.org/10.1146/annurev-marine-010419-010956

Cullen, J. J. (1982). The deep chlorophyll maximum: Comparing vertical profiles of chlorophyll a. *Canadian Journal of Fisheries and Aquatic Sciences*, *39*(5), 791–803. https://doi.org/10.1139/f82-108

Cullen, J. J. (2015). Subsurface chlorophyll maximum layers: Enduring enigma or mystery solved? *Annual Review of Marine Science*, *7*(1), 207–239. https://doi.org/10.1146/annurev-marine-010213-135111

Feldman, G., Clark, D., & Halpern, D. (1984). Satellite color observations of the phytoplankton distribution in the eastern equatorial pacific during the 1982-1983. El Niño. *Science*, *226*(4678), 1069–1071. https://doi.org/10.1126/science.226.4678.1069

Gelaro, R., McCarty, W., Suárez, M. J., Todling, R., Molod, A., Takacs, L., et al. (2017). The Modern-Era Retrospective analysis for Research and applications, version 2 (MERRA-2). *Journal of Climate*, *30*(14), 5419–5454. https://doi.org/10.1175/JCLI-D-16-0758.1

Gregg, W. W. (2008). Assimilation of seawifs ocean chlorophyll data into a three-dimensional global ocean model. *Journal of Marine Systems*, *69*(3), 205–225. (Physical-Biological Interactions in the Upper Ocean). https://doi.org/10.1016/j.jmarsys.2006.02.015

Gregg, W. W., & Casey, N. W. (2007a). Modeling coccolithophores in the global oceans. *Deep Sea Research Part II: Topical Studies in Oceanography*, *54*(5), 447–477. (The Role of Marine Organic Carbon and Calcite Fluxes in Driving Global Climate Change, Past and Future). https://doi.org/10.1016/j.dsr2.2006.12.007

Gregg, W. W., & Casey, N. W. (2007b). Sampling biases in modis and seawifs ocean chlorophyll data. *Remote Sensing of Environment*, *111*(1), 25–35. https://doi.org/10.1016/j.rse.2007.03.008

Gregg, W. W., & Casey, N. W. (2009). Skill assessment of a spectral ocean–atmosphere radiative model. *Journal of Marine Systems*, *76*(1), 49–63. https://doi.org/10.1016/j.jmarsys.2008.05.007

Gregg, W. W., Casey, N. W., & Rousseaux, C. S. (2014). Sensitivity of simulated global ocean carbon flux estimates to forcing by reanalysis products. *Ocean Modelling*, *80*, 24–35. https://doi.org/10.1016/j.ocemod.2014.05.002

Gregg, W. W., Ginoux, P., Schopf, P. S., & Casey, N. W. (2003). Phytoplankton and iron: Validation of a global three-dimensional ocean biogeochemical model. *Deep Sea Research Part II: Topical Studies in Oceanography*, *50*(22), 3143–3169. https://doi.org/10.1016/j.dsr2.2003.07.013

Greg Mitchell, B., & Kiefer, D. A. (1988). Chlorophyll α specific absorption and fluorescence excitation spectra for light-limited phytoplankton. *Deep-Sea Research, Part A: Oceanographic Research Papers*, *35*(5), 639–663. https://doi.org/10.1016/0198-0149(88)90024-6

IOCCG. (2008). *Why ocean colour? The societal benefits of ocean-colour technology*. In T. Platt, N. Hoepffner, V. Stuart, & C. Brown (Eds.) (Vol. No. 7). Author. https://doi.org/10.25607/OBP-97

IOCCG. (2020). *Synergy between ocean colour and biogeochemical/ecosystem models*. In S. Dutkiewicz (Ed.) (Vol. No. 19). Author. https://doi.org/10.25607/OBP-711

Johnson, K. S., Plant, J. N., Coletti, L. J., Jannasch, H. W., Sakamoto, C. M., Riser, S. C., et al. (2017). Biogeochemical sensor performance in the SOCCOM profiling float array. *Journal of Geophysical Research: Oceans*, *122*(8), 6416–6436. https://doi.org/10.1002/2017jc012838

Kuhn, A. M., Mazloff, M., Dutkiewicz, S., Jahn, O., Clayton, S., Rynearson, T., & Barton, A. D. (2023). A global comparison of marine chlorophyll variability observed in Eulerian and Lagrangian perspectives. *Journal of Geophysical Research: Oceans*, *128*(7), e2023JC019801. https://doi.org/10.1029/2023JC019801

Landschützer, P., Gruber, N., & Bakker, D. C. E. (2016). Decadal variations and trends of the global ocean carbon sink. *Global Biogeochemical Cycles*, *30*(10), 1396–1417. https://doi.org/10.1002/2015GB005359

Laufkötter, C., Vogt, M., Gruber, N., Aita-Noguchi, M., Aumont, O., Bopp, L., et al. (2015). Drivers and uncertainties of future global marine primary production in marine ecosystem models. *Biogeosciences*, *12*(23), 6955–6984. https://doi.org/10.5194/bg-12-6955-2015

Marinov, I., Gnanadesikan, A., Toggweiler, J., & Sarmiento, J. L. (2006). The Southern Ocean biogeochemical divide. *Nature*, *447*(7096), 964–967. https://doi.org/10.1038/nature04883

Martin, J., Gordon, R. M., & Fitzwater, S. E. (1990). Iron in Antarctic waters. *Nature*, *345*(6271), 156–158. https://doi.org/10.1038/345156a0

Matsumoto, G. I., Johnson, K. S., Riser, S., Talley, L., Wijffels, S., & Hotinski, R. (2022). The global ocean biogeochemistry (GO-BGC) array of profiling floats to observe changing ocean chemistry and biology. *Marine Technology Society Journal*, *56*(3), 122–123. https://doi.org/10.4031/MTSJ.56.3.25

McKee, D. C., Doney, S. C., Della Penna, A., Boss, E. S., Gaube, P., Behrenfeld, M. J., & Glover, D. M. (2022). Lagrangian and Eulerian time and length scales of mesoscale ocean chlorophyll from bio-argo floats and satellites. *Biogeosciences*, *19*(24), 5927–5952. https://doi.org/10.5194/bg-19-5927-2022

Oort, A. (1983). Global atmospheric circulation statistics, 1958-1973. (Tech. Rep.). *NOAA professional paper 14*.

Park, J.-Y., Stock, C. A., Dunne, J. P., Yang, X., & Rosati, A. (2019). Seasonal to multiannual marine ecosystem prediction with a global earth system model. *Science*, *365*(6450), 284–288. https://doi.org/10.1126/science.aav6634

Proctor, C. W., & Roesler, C. S. (2010). New insights on obtaining phytoplankton concentration and composition from in situ multispectral chlorophyll fluorescence. *Limnology and Oceanography: Methods*, *8*(12), 695–708. https://doi.org/10.4319/lom.2010.8.0695

Rienecker, M. M., Suarez, M. J., Gelaro, R., Todling, R., Bacmeister, J., Liu, E., et al. (2011). MERRA: NASA's Modern-Era Retrospective analysis for Research and applications. *Journal of Climate*, *24*(14), 3624–3648. https://doi.org/10.1175/JCLI-D-11-00015.1

Riser, S. C., Swift, D., & Drucker, R. (2018). Profiling floats in soccom: Technical capabilities for studying the southern ocean. *Journal of Geophysical Research: Oceans*, *123*(6), 4055–4073. https://doi.org/10.1002/2017JC013419

Riser, S. C., Talley, L. D., Wijffels, S. E., Nicholson, D., Purkey, S., Takeshita, Y., et al. (2023). SOCCOM and GO-BGC float data—snapshot 2022-12-21. In *Southern Ocean carbon and climate observations and modeling (SOCCOM) and global ocean biogeochemistry (GO-BGC) biogeochemical-argo float data archive*. UC San Diego Library Digital Collections. https://doi.org/10.6075/J0NS0V3Z

Roesler, C., Uitz, J., Claustre, H., Boss, E., Xing, X., Organelli, E., et al. (2017). Recommendations for obtaining unbiased chlorophyll estimates from in situ chlorophyll fluorometers: A global analysis of wet labs eco sensors. *Limnology and Oceanography: Methods*, *15*(6), 572–585. https://doi.org/10.1002/lom3.10185

Rousseaux, C. S., & Gregg, W. W. (2012). Climate variability and phytoplankton composition in the Pacific Ocean. *Journal of Geophysical Research*, *117*(C10), C10006. https://doi.org/10.1029/2012JC008083

Rousseaux, C. S., & Gregg, W. W. (2015). Recent decadal trends in global phytoplankton composition. *Global Biogeochemical Cycles*, *29*(10), 1674–1688. https://doi.org/10.1002/2015GB005139

Sarmiento, J. L., Gruber, N., Brzezinski, M. A., & Dunne, J. P. (2004). High-latitude controls of thermocline nutrients and low latitude biological productivity. *Nature*, *427*(6969), 56–60. https://doi.org/10.1038/nature02127

Schallenberg, C., Strzepek, R. F., Bestley, S., Wojtasiewicz, B., & Trull, T. W. (2022). Iron limitation drives the globally extreme fluorescence/chlorophyll ratios of the southern ocean. *Geophysical Research Letters*, *49*(12), e2021GL097616. https://doi.org/10.1029/2021GL097616

Schopf, P. S., & Loughe, A. (1995). A reduced-gravity isopycnal ocean Model: Hindcasts of El Niño. *Monthly Weather Review*, *123*(9), 2839–2863. https://doi.org/10.1175/1520-0493(1995)123⟨2839:ARGIOM⟩2.0.CO;2